BULLETIN OF THE CHEMICAL SOCIETY OF JAPAN, VOL. 46, 3671—3676 (1973)

Kinetics of Hydrogen Electrode Reaction on Mercury. II. Experimental Part. Elucidation of Non-steady State by Constant Potential and Linear Potential-sweep Methods

Akiko Katayama and Hideaki Kita
Research Institute for Catalysis, Hokkaido University, Sapporo 060

(Received July 2, 1973)

Potentiostatic and potentiodynamic experiments on Hg in 1 M HCl, HBr, and HI solutions were carried out to elucidate transient phenomena of the electrochemical mechanism of the hydrogen electrode reaction. The results obtained by both methods agree with the analysis of the non-steady state based on the electrochemical mechanism. The large effect of anions on the transient phenomena is satisfactorily interpreted by the change of repulsive force energy between $H_2^+(a)$'s on electrode, which is caused by the presence of specifically adsorbed anions in various degrees. The potential-sweep method reveals features of the step preceding the rate-determining step and gives the value of the repulsive force energy between $H_2^+(a)$'s as expected by the analysis.

We have theoretically discussed transient phenomena of the hydrogen electrode reaction(HER) on mercury on the basis of the electrochemical mechanism.[1] It was found that in relaxation methods the steady state condition can not be fulfilled at low overvoltages and that the linear potential-sweep will reveal Tafel plots with the current plateau characteristic of adsorption process.

A tendency to the current plateau, known as "depolarization", has been reported on a hanging electrode in H_2SO_4 solution by the galvanostatic method[2] and on DME in acidic KI solutions.[3] Tza and Iofa[3] interpreted the tendency by tacitly assuming a steady state of the reaction. However, the steady state assumption cannot predict either S-type Tafel plots or the dependence of the current plateau on the sweep rate.

The present work has been carried out to test experimentally these predictions and verify our fundamental assumption of the non-steady state of the reaction. A few analyses on the non-steady state have been reported; Horiuti and Okamoto[4] discussed HER

---

[1] A. Katayama and H. Kita, Part I, This Bulletin, **46**, 3665 (1973).

[2] O. Nagashima and H. Kita, *J. Res. Inst. Catal. Hokkaido Univ.*, **15**, 49 (1967).

[3] Tza Chuan-sin and Z. A. Iofa, *Dokl. Akad. Nauk U.S.S.R.*, **126**, 1308 (1959).

[4] J. Horiuti and G. Okamoto, This Bulletin, **13**, 216 (1938).

on Ni and Gerischer and Mehl[5] on Hg, Ag, and Cu. However, both works were restricted to a qualitative discussion. The latter authors applied only a constant overvoltage of 1.0 V to Hg electrode in 1/2 M H_2SO_4 solution and hence, though they did not observe the time-dependent current, their work is not sufficient to deduce the nature of the non-steady state.

We have applied the pulses of various constant overvoltages and of linear potential-sweep with different sweep rates to Hg electrode in acidic solutions. The resulting current-time or current-potential curves were compared with the predictions from the non-steady state analysis.

Experimental

Cell. An H-type cell of Pyrex was used; DME served as a test electrode.[6] The cell was kept in a water-bath whose temperature was controlled at 30±0.01 °C. The resistance of mercury column of DME was 58 ohms.

Solutions, Gas, and Mercury. 1 M solutions of HCl, HBr, HI, KCl, KBr, and KI were used. They were prepared from reagents of special grade and the water was purified as follows. The water from a Cu still was again distilled over alkaline $KMnO_4$ in a Pyrex flask furnished on top with a glass tube full of glass beads heated at 100 °C. The water vapor thus fractionally distilled was passed through a quartz tube heated at 450 °C for the protection of the creeping of water film along the wall. Commercial H_2 gas was purified through a permeation-type purifier of Japan Pure Hydrogen Co. The purified H_2 was introduced through a liquid N_2 trap and a bubbler of the distilled water into both compartments of the cell in order to deaerate and saturate the solution with H_2. Bubbling in the compartment of DME was stopped during measurements. Mercury flow rate of DME was 1.23 mg/s.

Electrical circuits. Pulse of constant potential or linear potential-sweep was applied to a growing Hg drop through a potentiostat. The τ_1, the time when the pulse was imposed and τ_2, a drop life time were controlled respectively at 3.6 and 4.0 s by Tektronix 160 series Generators with a device of mechanical knocking. Figure 1 shows a basic circuit of the potentiostat with a current transducer of operational amplifier, OP–C. The power supply for the potentiostat was made by Teledyne 825 Du Voltage Regulators.

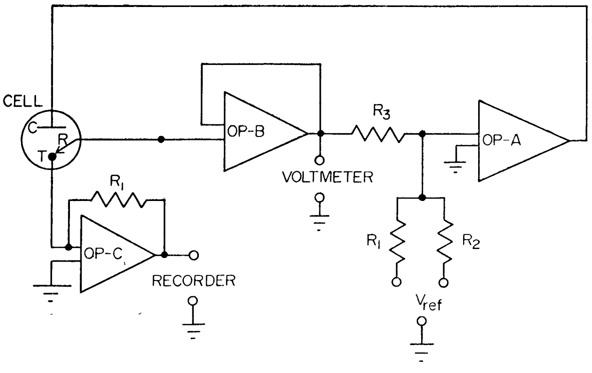

Fig. 1. Block diagram of potentiostat.
OP-A and C, Operational amplifier of Teledyne Type 1301; OP-B, Teledyne Type QFT-2B; R's resistance ($R_1=R_2=R_3$, and R_i changeable); T, R, and C, test, reference, and counter electrodes.

DME was initially kept at an overvoltage η_1 by Takasago DC power Supply GPO-2 through the potentiostat. After DME was kept at η_1 for τ_1 s, pulses of constant or sweeping potential from Hewlett Packard Function Generator 3300A with Plug-in Unit of 3302A were applied through the potentiostat. The width of the pulse Δt was limited by $\Delta t<\tau_2-\tau_1$. Since the area of DME, A is proportional to $(mt)^{2/3}$ at a constant flow rate of mercury m, the increase of drop area ΔA during Δt is given by

$$\frac{\Delta A}{A}=\frac{\{m(\tau_1+\Delta t)\}^{2/3}-(m\tau_1)^{2/3}}{(m\tau_1)^{2/3}}\simeq\frac{2\Delta t}{3\tau_1} \qquad (1)$$

The last member of Eq. (1) holds when $\Delta t \ll \tau_1$.

Measurements. Δt was always less than 0.1 ms. Therefore, $\Delta A/A$ was less than 2%. Overvoltage of DME was η_1 at $\tau=0\sim\tau_1$ and then $\eta(>\eta_1)$ at τ_1, where η's were defined at the negative of the electrode potential referred to reversible hydrogen electrode. All measurements with HI and KI solutions were performed in the dark.

Results

(A) Constant Potential Method. Current *vs.* time ($I-t$) curves are observed for various η in 1 M HCl (Fig. 2, $\eta_1=0$), 1 M HBr (Fig. 3, $\eta_1=0$), and 1 M HI

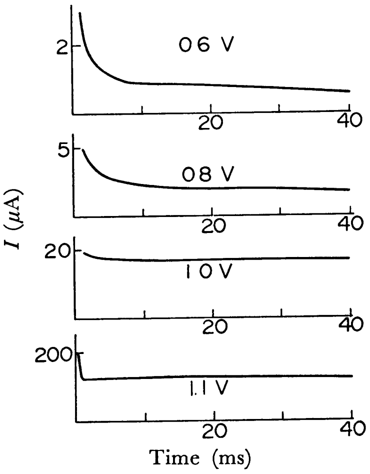

Fig. 2. Current *vs.* time curves for various overvoltages in 1 M HCl solution when $\eta_1=0$ V.

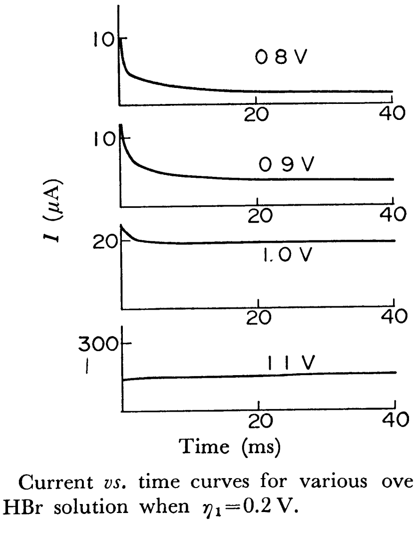

Fig. 3. Current *vs.* time curves for various overvoltages in 1 M HBr solution when $\eta_1=0.2$ V.

---

[5] H. Gerischer and N. Mehl, *Z. Elektrochem.*, **59**, 1049 (1955).
[6] A. Katayama and H. Kita, *Chem. Lett.*, **1973**, 359.

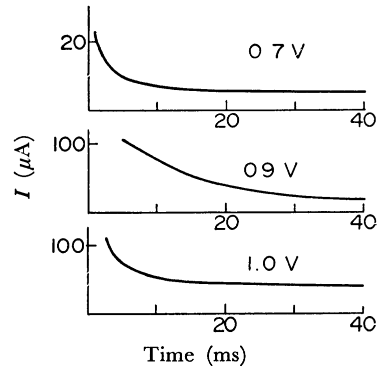

Fig. 4. Current *vs.* time curves for various overvoltages in 1 M HI solution when $\eta_1=0.2$ V.

(Fig. 4, $\eta_1=0.2$ V) where t is counted from τ_1. As these figures have a common time scale, we can easily find effects of the overvoltage and electrolyte on $I—t$ curve. Each figure shows a similar overvoltage effect; a decay of I with t is weakened with the increase of η and at sufficiently high overvoltages I seems to be time-independent. This decay can not be attributed to an effect of the charging of double layer, since the time constant of the charging is less than 0.05 ms. As regards the electrolyte effect, the decay of I is enhanced in the order HI>HBr>HCl. $I—t$ curves observed on the electrode initially polarized with various η_1 are compared in Fig. 5. Current tends to reach earlier a constant common value when η_1 is increased. This is in line with the theoretical analysis; the coverage of $H_2^+(a)$, θ, at high η_1 is estimated to be close to a limiting value, so that the current will more rapidly reach a steady value.

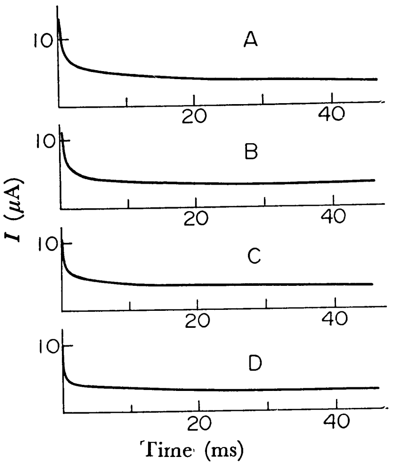

Fig. 5. Current *vs.* time curves at $\eta=0.9$ V in 1 M HBr solution, when (A) $\eta_1=0$, (B) 0.2 V, (C) 0.3 V, and (D) 0.4 V.

Logarithms of the current density at $t=40$ ms (the longest time) are plotted against η in Fig. 6. At high overvoltages log i *vs.* η curves for various acidic solutions converge into one straight line with a slope of *ca.* 120 mV. However, at lower overvoltages, deviation from the straight line appears first in 1 M HI solution, then 1 M HBr and 1 M HCl solutions. This deviation is known as depolarization. It should be emphasized that the curves reveal an S-type behavior with a current plateau, though the latter is somewhat gradated.

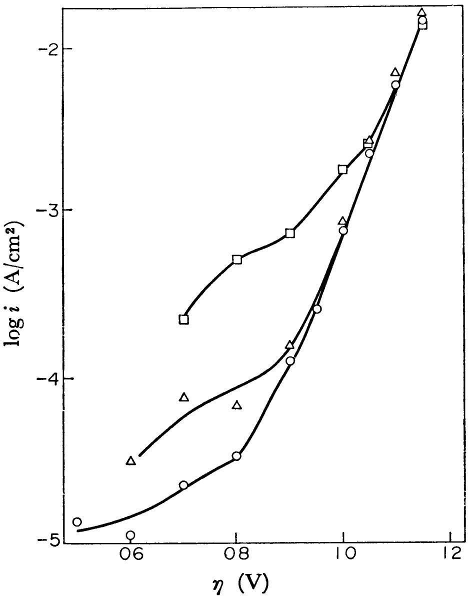

Fig. 6. Logarithm of current density at 40 ms *vs.* overvoltage.
○, 1 M HCl; △, 1 M HBr; □, 1 M HI.

Close examination of Fig. 6 in comparison with Figs. $2\sim4$ shows that the S-region of log i *vs.* t curves has a different feature in $I—t$ curves of Figs. 2—4 from those in the region of a straight line. In the S-region, I continues to decrease with t, but in the other, I remains constant from the begining. Thus, the appearance of the S-type behavior will prove that the reaction is in a non-steady state. In the region of a straight line, the reaction has already attained a steady state. The upward deviation from the straight line, *i.e.*, the depolarization, is simply due to the fact that the current in a non-steady state is always larger than that in a steady state. The results of Figs. 2—5 satisfy the predictions in Part I.

The degree of depolarization is found to be the largest in HI and the least in HCl solution. This is interpreted by the theoretical analysis1) as follows. The halide ions are known to be specifically adsorbed on the electrode surface in the order $I^->Br^->Cl^-$. Since the charge of these ions is opposite to that of the intermediate $H_2^+(a)$, adsorbed halide ions will reduce a coulombic repulsive force between $H_2^+(a)$'s in conformity with the degree of specific adsorption of these anions. Thus, $H_2^+(a)$'s in iodide solution have the least repulsive force. Our non-steady state analysis has predicted that the smaller the repulsive force between $H_2^+(a)$'s, the longer the time is required for a steady state to be attained. Consequently, the largest degree of depolarization is expected in iodide solution. The effect of halide ions on the depolarization is thus explained by the change of repulsive force between $H_2^+(a)$'s owing to their specific adsorption.

(B) Linear Potential-sweep Method. *(1) Neutral Solutions*: In neutral solutions, mercury electrode holds its ideally polarized state down to *ca.* −1.5 V

vs. NHE.[7] When the pulse of a linear potential-sweep is applied to the ideally polarizable electrode, the current observed consists of only the charging current of the double layer at an interface, I_{dl}, and satisfies the following relation with the sweep rate, v,

$$I = I_{\text{dl}} = C_{\text{dl}}v, \tag{2}$$

where C_{dl} is double layer capacity.

Figures 7∼9 show the double layer capacity calculated by the use of Eq. (2) for various v's in solutions of 1 M KCl, KBr, and KI, respectively. The values of C_{dl} are almost independent of v, except in 1 M KBr (Fig. 8) where at high overvoltages they deviate somewhat in a systematic way. It can be stated that this deviation is not caused by the desorption process of Br^-, since Lorenz[8] has shown that its desorption occurs at more positive potentials in a reversible way. Hence, it must be ascribed to some other processes. Nevertheless, the deviation does not give any serious effect on the following treatment. Figures 7∼9 give a double layer capacity almost identical to that measured by AC bridge.[3,7] The double layer is known to be dependent on the kind of anion but independent of a cation (H^+ or K^+). Such a dependence, however, vanishes at sufficiently negative potentials (Figs. 7∼9). Specifically adsorbed anions are considered to be absent at those negative potentials.

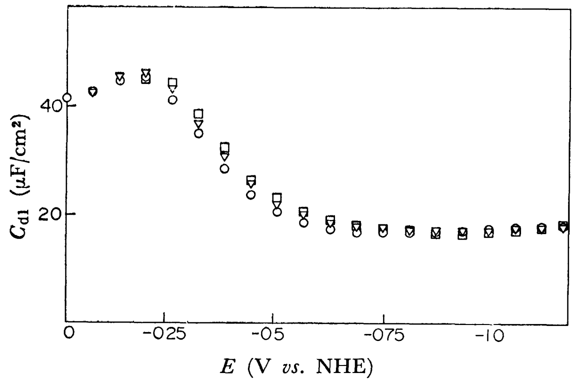

Fig. 7. Double layer capacity *vs.* potential curves for various sweep rates in 1 M KCl solution.
○: 46.4 V/s, ▽: 116 V/s, □: 232 V/s, each symbol was traced from oscilloscope screen.

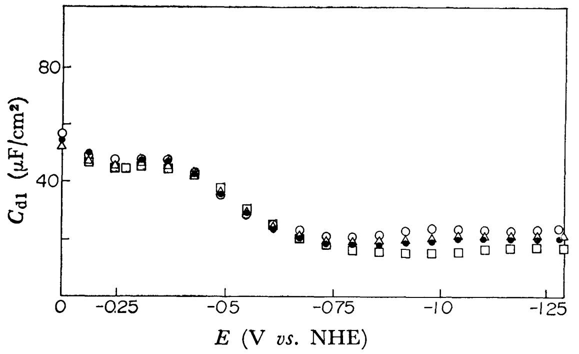

Fig. 8. Double layer capacity *vs.* potential curves for various sweep rates in 1 M KBr solution.
○: 11.6 V/s, △: 23.2 V/s, ●: 46.4 V/s, □: 232 V/s, each symbol was traced from oscilloscope screen.

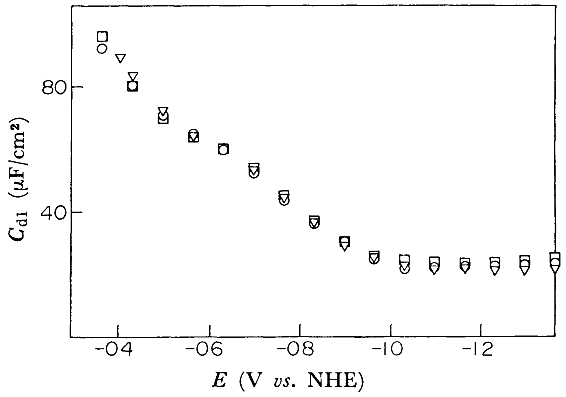

Fig. 9. Double layer capacity *vs.* potential curves for various sweep rates in 1 M KI solution.
○: 11.6 V/s, □: 46.4 V/s, ▽: 232 V/s, each symbol was traced from oscilloscope screen.

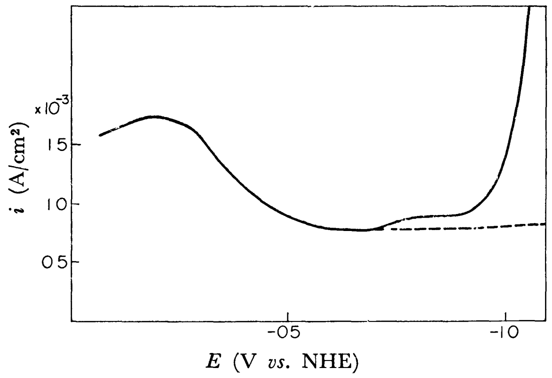

Fig. 10. Current *vs.* potential curves for sweep rate of 46.4 V/s.
Solid line, 1 M HCl; dotted line, 1 M KCl.

Thus, the currents observed in neutral solutions were used for the purpose of excluding I_{dl} from the observed one in the respective hydrogen halide solutions in which HER takes place.

(2) Acidic Solutions: Figure 10 shows typical i *vs.* potential E curves obtained at the same sweep rate in 1 M HCl and KCl solutions, where i represents the current density in A/cm². Those in 1 M HBr and HI solutions were described elsewhere.[6] The reaction current density i_r is equated by $(i - i_{\text{dl}})$, where i_{dl} is given by the current with the same sweep rate in neutral solution having the common anion. It is plausible that the double layer capacity does not undergo a change by the change of the solution from 1 M KCl to 1 M HCl, since Frumkin *et al.*[9] obtained the same double layer capacities by AC bridge method both in HCl and LiCl solutions, even though HER takes place in HCl solutions.

i_r thus obtained does not show a monotonous increase with η, but a plateau on the way of η increase. We shall call it a current plateau and denote its value at a flat portion by i_p. Values of i_p in HCl, HBr, HI solutions are found to be in the order $i_p\,(\text{HCl}) \lesssim i_p(\text{HBr}) \ll i_p(\text{HI})$. $i_p(\text{HCl})$ and $i_p(\text{HBr})$ are relatively

---

[7] D. C. Grahame, *Chem. Revs.*, **41**, 441 (1947).
[8] W. Lorenz, *Z. Phys. Chem.*, **224**, 145 (1964).
[9] A. N. Frumkin, O. A. Petry, and N. V. Nikolaeva-Fedorovich, *Dokl. Akad. Nauk U.S.S.R.*, **137**, 896 (1961).

small compared with i_{dl}, but i_p(HI) is much larger than i_{dl}.

Figures 11∼13 show log i_r *vs.* η plots for various sweep rates in 1 M HCl, HBr, and HI solutions. It is to be noted that the current at a flat portion i_p is almost independent of the sweep rate in 1 M HCl, but increases in 1 M HI solution. In the latter case, i_p at sweep rates of 11.6 V/s and 23.2 V/s is proportional to the sweep rate. The proportionality is what was predicted[1] by non-steady state analysis. Potential drop through a Hg column of DME is corrected at high current density in 1 M HI solution. Figure 14 shows the dependence of i_p of 1 M HI on the sweep rate in logarithmic scale, where we find a depression in its dependence from the proportional one when the sweep rate is large.

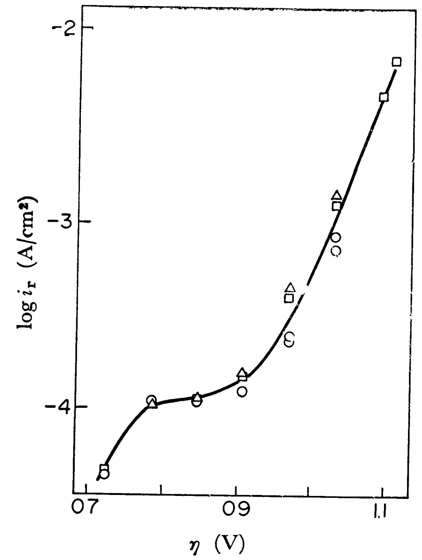

Fig. 11. Logarithm of reaction current *vs.* overvoltage in 1 M HCl by potential-sweep.
A: 11.6 V/s, ○, 23.2 V/s, □: 46.4 V/s.

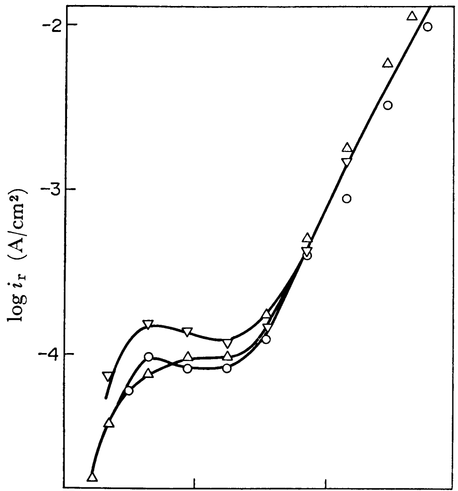

Fig. 12. Logarithm of reaction current *vs.* overvoltage in 1 M HBr by potential-sweep.
△: 11.6 V/s, ○: 23.2 V/s, ▽: 46.4 V/s.

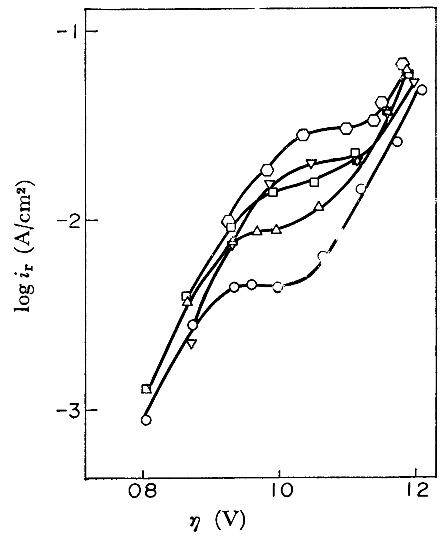

Fig. 13. Logarithm of reaction current *vs.* overvoltage in 1 M HI by potential-sweep.
○: 11.6 V/s, △: 23.2 V/s, □: 46.4 V/s, ▽: 116 V/s, ⬡: 232 V/s.

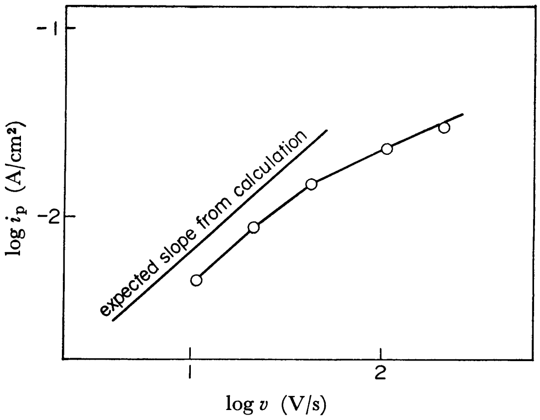

Fig. 14. Logarithm of plateau current *vs.* logarithm of sweep rate curve in 1 M HI.

This dependence of i_p on the kind of anion and on the sweep rate can be interpreted as follows.

i) Dependence of i_p on the kind of anion: Values of i_p in the respective solutions are in the same order as the degree of the specific adsorption of these anions. The current plateaus appear around overvoltages of 0.8 and 1.0 V in 1 M HCl and HI solutions (Figs. 11 and 13) and the double layer capacities at the corresponding potentials are 18 and 22 μF/cm² (Figs. 7 and 9), respectively. The value 18 μF/cm² is the same as that of the ideally polarized electrode, indicating the absence of the specifically adsorbed Cl^-. On the contrary, the latter value of C_{dl} in HI solution indicates the presence of specifically adsorbed I^- at potentials where i_p is observed.[6] Enhancement in i_p by the change of anion from Cl^- to I^- is clearly due to the specific adsorption of I^-.

The adsorbed anion is expected to reduce the effective charge of H_2^+(a)'s and hence to increase the coverage H_2^+(a). The relation $i_p(I^-) \gg i_p(Br^-) \gtrsim i_p(Cl^-)$ is thus explained by the change of repulsive force between H_2^+(a)'s. We can estimate the repulsive energy constant R_e from i_p[1]; at a sweep rate of 11.6 V/s, $R_e=$ 14 eV for 1 M HCl and HBr solutions and $R_e=0.28$ for 1 M HI solution where pseudocapacities are obtained as 12 μF/cm² and 600 μF/cm², respectively.

ii) Dependence of i_p on the sweep rate: i_p is expected to be proportional to the sweep rate, in which we have assumed that the repulsive force between $H_2^+(a)$'s is invariable irrespective of applied potentials. However, since the specific adsorption of anions varies with applied potentials, the repulsive force between $H_2^+(a)$'s should change with the change of the applied potential.

The current plateau appears at a more negative potential when the sweep rate is increased (Fig. 13). At more negative potentials, the repulsive force between $H_2^+(a)$'s increases because of the desorption of anions which act to reduce the $H_2^+(a)$'s repulsive force. As a consequence, i_p does not increase as expected from the proportional relationship with the sweep rate. In HCl and HBr solutions, i_p is smaller than i_{dl} and the subtraction of i_{dl} from i brings a relatively large error in i_p. We consider that this uncertainty in i_p is one reason for i_p in HCl and HBr appearing not to have a clear dependence on v.

Log i_r *vs.* η curves at more negative potentials than those in the region of the current plateau are independent of the sweep rate and become a single straight line, which agrees with the straight line mentioned in (A). We therefore infer that this portion represents the relation at a steady state.

Discussion

Employing the expression for the velocity of HER on Hg[1] and the repulsive energy constants in the previous section, (B)–(2)–(i), we simulated the values of rate constants so that the experimental Tafel plots at high overvoltages were reproduced. The rate of the step preceding the rate-determining one was found to be faster than the latter by three orders of magnitude in the case of *e.g.*, Fig. 13. The fitting rate constants are $k_2=10^{-18}\ s^{-1}\ cm^{-2}$ and $k_1=10^{-15}\ s^{-1}\ cm^{-2}$. From values of the repulsive energy constant and the rate constants, we can estimate the time required for the steady state to be attained when a constant potential is applied. The results are shown in Table 1, where the other parameters not listed are identical to those given previously.[1] Thus, the time required strongly depends on the repulsive energy constant between $H_2^+(a)$'s.

TABLE 1. THE TIME REQUIRED FOR A STEADY STATE TO BE ATTAINED

η	Time (s)		
	$R_e=13.35$ eV	2.67 eV	0.534 eV
0.1 V	1.7×10^4		
0.2	1.2×10^4	2.5×10^4	$>6\times10^4$
0.3	4.9×10^3		
0.4	6.5×10^2	$>1.2\times10^3$	
0.5	90		
0.6	20	$>1.8\times10^2$	
0.7	2		

$k_1=10^{-15}\ s^{-1}\ cm^{-2}$, $k_2=10^{-18}\ s^{-1}\ cm^{-2}$.

The explanation for depolarization by Tza and Iofa[3] is based on the steady state assumption and only successful in the relatively negative potential regions where depolarization is small. The S-type Tafel plots can be explained only as a transient phenomena where the reaction stays in non-steady state, as demonstrated by the present two methods. Our observation at an overvoltage of 1.0 V in 1 M HCl is very analogous to that in 0.5 M H_2SO_4 by Gerischer and Mehl,[5] although their conclusion is contradictory to ours since their observation was limited only to a value of 1.0 V.

No pH dependence of double layer capacity observed by 1 kHz AC bridge could be taken as an evidence for the exclusion of the electrochemical mechanism,[9] since the presence of the reversible step of $2H^++e^-\rightleftarrows H_2^+(a)$ should rise to the additional pseudocapacity which is pH dependent. However, we have found that the rate of this step is so small in its absolute magnitude that it can not follow the rapid variation of voltages such as 1 kHz AC. Moreover, the repulsive force between $H_2^+(a)$'s is so large that θ reaches a limiting value by the very small increase. The change of coverage in HCl and HBr solutions is at maximum $\Delta\theta=2\times10^{-3}$, which was obtained from observed i_p's and theoretical analysis. Such a small $\Delta\theta$ can not be detected by AC bridge. Thus, the observation with 1 kHz AC provides only information on the intrinsic double layer capacity as seen in (B)—(1) in the previous section. However, in HI solution, i_p is markedly large in comparison with that in HCl and HBr solutions; $\Delta\theta$ amounts to 0.65 at maximum.

A striking effect of the specific adsorption of anion on transient phenomena of HER is the strong evidence for the assumption that the intermediate possesses a charge; namely the fact that the adsorbed anion reduces the repulsive force among intermediates, strongly suggests positively charged intermediate such as $H_2^+(a)$ in the electrochemical mechanism.